Cellulose Thin Films: Degree of Cellulose Ordering and Its Influence on Adhesion

Malin Eriksson,[‡] Shannon M. Notley,[§] and Lars Wågberg*[,†]

Department of Fibre and Polymer Technology, School of Chemical Science and Engineering, KTH, Royal Institute of Technology, SE-100 44 Stockholm, Sweden, Carmeda AB, Kanalvägen 3B, SE-194 61 Upplands Väsby, Sweden, and Department of Applied Mathematics, Research School of Physical Sciences and Engineering, Australian National University, Canberra 0200 ACT, Australia

Received December 8, 2006; Revised Manuscript Received January 15, 2007

Adhesion measurements have been performed with thin cellulose films using continuum contact mechanics with application of the JKR theory. Three different cellulose surfaces were prepared, one crystalline and two surfaces with a lower degree of crystalline order. Adhesion between two cross-linked poly(dimethylsiloxane) (PDMS) caps, as well as the adhesion between PDMS and the various cellulose surfaces, was measured. The work of adhesion (from loading) was found to be similar for all three surfaces, and from contact angle measurement with methylene iodide it was concluded that dispersive interactions dominate. However, the adhesion hysteresis differed significantly, being larger for a less ordered cellulose surface and decreasing with increasing degree of crystalline order. This is suggested to be due to the surface groups' ability to orient themselves and participate in specific or nonspecific interactions, where a surface with a lower degree of crystalline order has a higher possibility for reorientation of the surface groups. The mobility of cellulose chains increases with water uptake, resulting in stronger adhesive joints. These films will hence allow for determination of the contributions of hydrogen bonding and inter-diffusion on the adhesion, determined from the unloading data, as the thermodynamic work of adhesion was found to be independent of the cellulose surface used.

Introduction

Cellulose-based fibers are used in both paper and composite industries. Common for all of these applications is that the adhesion between the constituents will determine the mechanical properties of the final product. Naturally, the most commonly used method for determining the paper or the composite strength is to perform tensile testing.[1] These types of mechanical testing are of importance for evaluation of macroscopic properties. However, it is also important to study the molecular adhesion between the components in the paper/composite, as this provides information on the molecular scale regarding interactions between the surfaces.

To establish how cellulose surfaces join together and hold together, knowledge of the molecular adhesion force between cellulose surfaces and typical additives is of great interest. The work of adhesion between any two materials can be divided into specific interactions, for example, acid−base interactions and Lifshitz−van der Waals interactions.[2] It should be noted that traditional hydrogen bonding, in this terminology, is a specific example of an acid/base interaction. Simply stated, the acid/base interactions result in strong adhesion between an acidic surface and a basic surface, whereas weak adhesion is obtained between two surfaces with the same polarity. From contact angle measurements, it is possible to calculate surface energies of various surfaces, such as cellulose; using this information, the work of adhesion between two contacting surfaces can be estimated.[2] However, it is difficult to obtain information about acid and base properties of various surfaces, and there is still no unified theory available regarding polar interactions.[3] Experimental data from the use of well-characterized cellulose surfaces, which are smooth on a nanometer scale, and high resolution measuring techniques for determination of the adhesion between the surfaces will allow for elegant model experiments where the importance of electrostatic interactions, van der Waals interactions, hydrogen bonding, and inter-diffusion can be determined. This in turn will provide new insight in the preparation of chemically engineered wood-based materials.

There are many different types of flat cellulose surfaces and cellulose spheres available.[4−11] Because the raw material, the dissolution procedures, and the film preparation procedures do differ, it will be difficult to compare the measured interaction forces between such surfaces. Many interaction studies between cellulose surfaces in aqueous solutions have shown steric interactions either at short or at long distances.[7,8,11−13] This probably originates from the fact that the cellulose surfaces used in these studies were mainly amorphous and showed large tendency to swell in the used solvent. However, in two recent atomic force microscope (AFM) investigations, where spin-coated (SC) semicrystalline cellulose II surfaces were used together with a colloidal probe of hornified amorphous cellulose, van der Waals interactions were detected between the surfaces at low pH. The interaction between the cellulose surfaces at higher pH was dominated by electrostatic interactions.[10,14] Pure electrostatic interactions have also been detected between two cellulose spheres with the aid of AFM at elevated pH.[15] These differences in interaction profiles show the importance of preparation procedures and how this significantly affects the results.

Few studies have been performed under "dry" conditions. Holmberg et al.[7] used the surface force apparatus in combination

* Corresponding author. Telephone: +46 8-790 8294. Fax: +46 8-790 8101. E-mail: wagberg@polymer.kth.se.
† Royal Institute of Technology.
‡ Carmeda AB.
§ Australian National University.

10.1021/bm061164w CCC: $37.00
Published on Web 02/24/2007

with Langmuir Blodgett (LB) cellulose films, that is, amorphous surfaces, and were able to determine the work of adhesion between cellulose surfaces in both dry air and 100% relative humidity (RH). In dry air, the measured adhesion force varied between 500 and 1000 mN/m. The difference was ascribed to the small-scale roughness that still could be detected on the LB films. In moist air, that is, 100% RH, the work of adhesion was difficult to measure due to the capillary condensation between the surfaces. Continuum contact mechanics, using the JKR (Johnson Kendal and Roberts) approach,[16] has also been used for evaluation of adhesion to cellulose surfaces in ambient conditions. Adhesion between a cross-linked poly(dimethylsiloxane) (PDMS) and a LB-cellulose surface,[17] as well the cellulose II surface,[18] has been measured, both showing a distinct adhesion hysteresis, which has been suggested to be due to hydrogen bonding between the OH groups on the cellulose and the oxygen on the PDMS surface.[17]

There is an increasing interest in obtaining new information on the nature of the cellulose−cellulose interaction, with and without different types of additives present, and, as already mentioned, it is vital to have access to a representative cellulose surface for these studies. In the present work, the JKR approach was used to study the adhesion between PDMS and three cellulose surfaces, different with respect to their degree of crystalline order. From an earlier investigation by the authors, it was shown that forces acting between the cellulose surfaces in an aqueous environment are highly dependent on the type of cellulose surface used.[19] To complete these studies, it was decided to investigate how the preparation procedure of the cellulose surfaces would influence the adhesion under ambient conditions. Furthermore, the use of such cellulose films provides an excellent opportunity to study, on a molecular level, the importance of surface preparation, that is, the dissolution procedure and the resulting degree of crystalline ordering of prepared cellulose surfaces.

Materials

Polyvinyl amine (PVAm), supplied by BASF Germany, was used as the cationic anchoring polymer, that is, providing an adhering surface for the cellulose. NMMO (*N*-methylmorpholine *N*-oxide) supplied as a 50% (w/w) aqueous solution and methylene iodide were obtained from Aldrich, while dimethylsulfoxide (DMSO) was supplied by KeBo. LiCl and dimethylacetamide (DMAc) were supplied by Sigma-Aldrich. Milli-Q water was used in all experiments.

PDMS hemispherical caps were prepared from poly(dimethylsiloxane) (182 silicone elastomer, Dow Corning, U.S.) and a curing agent (182 curing agent silicone elastomer, Dow Corning, U.S.) as described previously.[18] The curing agent (1 part by weight) was added to the silicone elastomer (10 parts by weight) under vigorous stirring. To remove air bubbles, the mixture was treated under vacuum for 1 h. Droplets of the reaction mixture were placed on a glass slide treated with fluorodecyltrichlorosilane (Aldrich), and PDMS sheets were prepared by pouring the mixture into a Petri dish made of glass. The PDMS was then cured for 1 h at 105 °C. The cured caps/sheets were extracted in heptane for about 12 h to remove unreacted monomer. Finally, they were oxidized in a plasma cleaner (model PDC 002, Harrick Scientific Corp., NY) in air for different times ranging from 0 to 5 min at a power level of 7 W.

Silicon wafers (150 mm, p-type) were used as base-substrates for the cellulose surfaces and were purchased from Memc Electronics Materials, Novara, Italy. They were washed consecutively with ethanol and Milli-Q water, blown dry with nitrogen, and oxidized in a plasma cleaner.

A northern softwood dissolving grade pulp, Temalfa 93 (Tembec Inc., Temiscaming, Canada), was used to prepare a cellulose nanocrystal suspension by acid hydrolysis according to a previously described method (kindly provided by Derek Grey, McGill University, Montreal, Canada).[6] This colloidal suspension of cellulose I nanocrystals 3% (w/w) was spin-coated onto a silica wafer, pretreated with the PVAm, at 4000 rpm for 1 min. The films were subsequently heat treated at 90 °C for 4 h to remove most of the sulfate groups on the cellulose and to ensure that the films did not delaminate upon exposure to aqueous electrolyte solution. This procedure has previously been shown to produce cellulose I films as determined from X-ray diffraction.[6] The film thickness was approximately 120 nm according to ellipsometry measurements. A similar dissolving grade pulp from Domsjö Fabriker (Domsjö, Sweden) was used as the raw material for the preparation of cellulose thin films with less degree of order, (A) and (B), respectively. Before use, these fibers were extracted in acetone for 12 h.

The second type of cellulose surface was prepared according to Gunnars et al.[4,5] A cellulose solution was first prepared by dissolving 0.5 g of pulp in 25 g of NMMO at 115 °C for approximately 2 h. 75 g of DMSO was then added to the solution to decrease the viscosity before spin-coating to give a final cellulose solution concentration of 0.5% (w/w). Films were spin-coated at up to 3500 rpm for 30 s onto oxidized silicon wafers pretreated with an anchoring layer of PVAm. Finally, the films were solvent exchanged in Milli-Q water for 12 h, and the water was exchanged after 1 and 3 h. This produced films with a thickness of about 30 nm, as measured using ellipsometry. Earlier investigations using NMMO/DMSO for dissolving the cellulose raw material have been shown to produce regenerated cellulose consisting of about 50% crystalline cellulose II-type material.[20] These measurements of crystallinity[20] were conducted with fibers spun from NMMO solutions and not directly on the thin films. Because the method of regeneration of the cellulose might have an effect on the degree of ordering, the surfaces prepared from NMMO/DMSO solutions were denoted as surfaces with a lower degree of crystalline order and denoted as cellulose surface A so as not to give the false interpretation that the degree of crystallinity had been determined for these specific surfaces.

The third cellulose dissolution procedure for preparing cellulose surfaces was adapted without the derivatizing agent according to Berthold et al.,[21] and the film preparation followed the description by Eriksson et al.[9] 0.5 g of acetone extracted dissolving grade pulp was initially immersed in Milli-Q water to allow the pulp to swell. After 24 h, the pulp suspension was filtered to remove most of the water. The pulp was then placed into methanol for 30 min with stirring before filtering. This was repeated three times. The pulp was then solvent exchanged to DMAc by immersion for 30 min. This was repeated three times with filtration between each step. 1.5 g of LiCl was added to 18 mL of DMAc, which was heated to 110 °C. When a clear solution was obtained, the solution was removed from heat and allowed to cool. The solvent exchanged pulp was then added to the solution of LiCl in DMAc in small portions. The pulp was allowed to dissolve at room temperature for 24 h, after which a clear, colorless, but highly viscous cellulose solution was formed. This solution was subsequently diluted with 80 mL of DMAc (to a final cellulose concentration of 0.5% w/w) and heated to a temperature of 110 °C before spin-coating onto an oxidized silicon wafer pretreated with a cationic anchoring polymer layer. These cellulose surfaces were then placed into Milli-Q water to remove any excess LiCl and solvent before being blown dry with nitrogen. The dry thickness of the amorphous cellulose thin film was measured to be 44 nm using ellipsometry. Earlier studies using LiCl/DMAc for dissolving softwood pulp have shown to reduce or totally remove the degree of crystalline ordering significantly.[22] Actually, the results showed[22] that the regenerated material consists of amorphous cellulose. However, because the method of the cellulose regeneration might have an effect on the degree of ordering, the surfaces prepared from LiCl−DMAc solutions were denoted as surfaces with a lower degree of crystalline order and as cellulose surface B so as not to give the false interpretation that the degree of crystallinity, that is, the lack of crystallinity, had been determined for these specific surfaces.

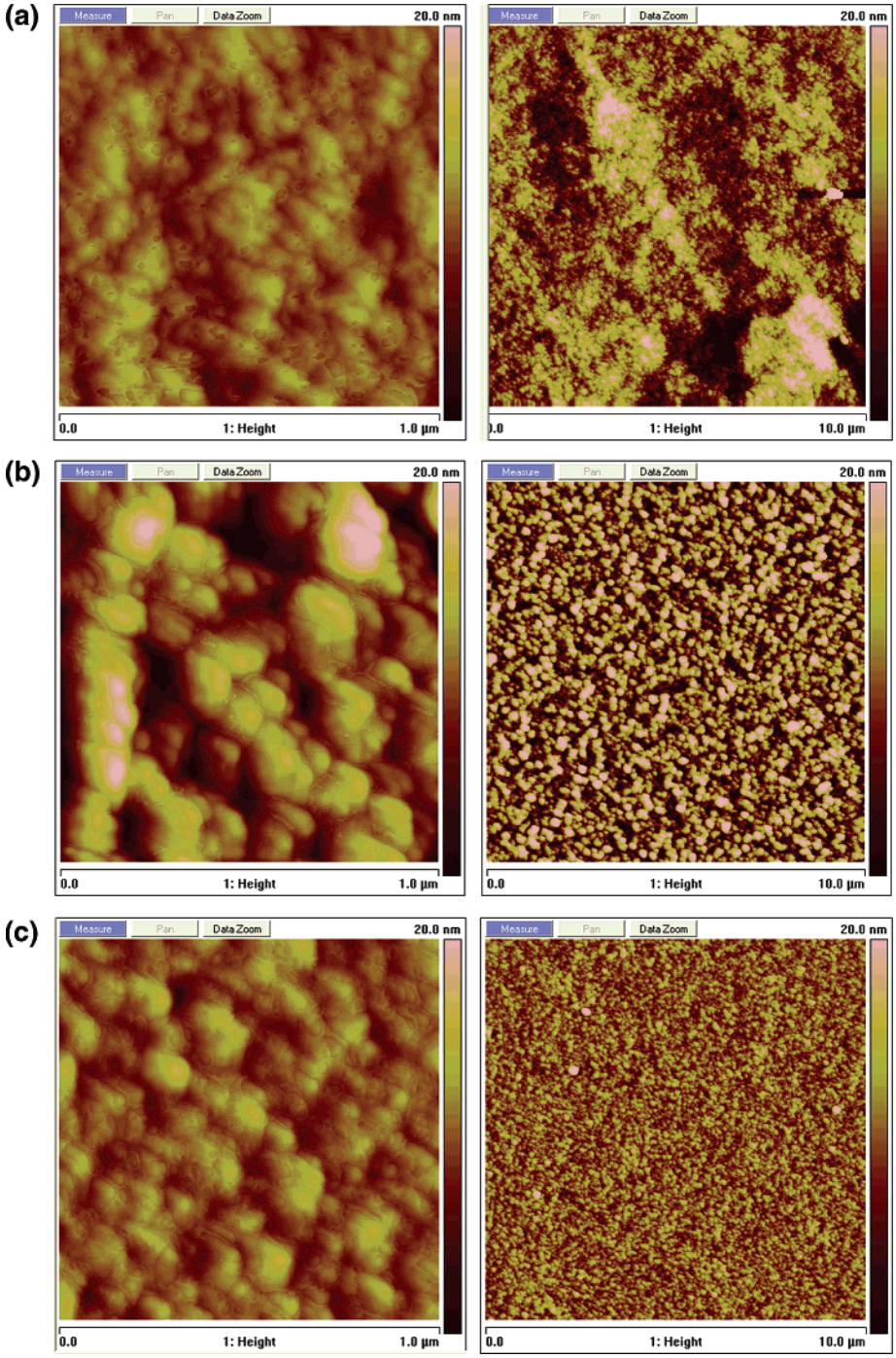

Figure 1. AFM tapping mode height images of cellulose thin films on silica. (a) Cellulose I, (b) cellulose A, and (c) cellulose B. The scanned surface areas were 1 μm^2 (left) and 100 μm^2 (right).

Methods

AFM Imaging. The prepared cellulose surfaces were imaged in tapping mode, using a Multimode scanning probe microscope (Veeco Ltd., Santa Barbara, CA). These images were used to derive rms (root-mean-square) values for each cellulose surface with aid of the Veeco software.

Contact Angle Measurements. Static contact angle measurements against Milli-Q water and methylene iodide were performed for the cellulose surfaces and PDMS sheets as well as oxidized PDMS (OxPDMS) sheets, using a KSV contact angle meter, CAM 200 (Helsinki, Finland). The values reported were taken after the contact angle had reached a stable value, typically less than 10 s after deposition of the droplet.

Ellipsometry Measurements. The ellipsometry measurements were performed using a Beaglehole scanning imaging ellipsometer (Beaglehole Instruments, Beaglehole, New Zealand). The thickness of the different cellulose films was determined from the measurement of the *x* and *y* parameters as the angle of incidence was varied between 65° and 80°. The model employed to fit the data was air/cellulose/silica/silicon, and all materials were assumed to be optically isotropic. The refractive indices of the materials were 3.8 (silicon) and 1.48 (silica). The calculations employed a least-squares iterative fitting procedure using both thickness and refractive index of the cellulose layer as fitting parameters. The measurements were performed under ambient air and relative humidity conditions. The ellipsometric measurements were repeated several times at different positions on the surface. The refractive index of the cellulose films was determined to be in the range of 1.54−1.58 in agreement with previous studies.[7]

Microadhesion Measurement Apparatus (MAMA). In a typical experiment with this equipment, an elastic lens (PDMS cap) is stepwise

Table 1. RMS Surface Roughness Values for the Different Cellulose Surfaces Measured in Areas of 1 and 100 μm^2

sample	rms value (nm) 1 μm^2	rms value (nm) 100 μm^2
cellulose I	2.3	3.1
cellulose A	3.9	5.7
cellulose B	1.9	2.5

Table 2. Contact Angles against Water and Methylene Iodide on Different Cellulose Surfaces and PDMS Sheets with an Error of ±2 (Literature Values Included)[a]

sample	water (deg)	methylene iodide (deg)	water (deg) literature values	methylene iodide (deg) literature values
cellulose I	19.5	34		
cellulose A	17	40	22[18]	39[18]
cellulose B	18	37		
PDMS	110	72	112 ± 2[33]	70[26]
OxPDMS	0	44	0[26]	

[a] OxPDMS was obtained by plasma treatments of PDMS in air for 1 min.

pressed toward the lower surface, containing a bare model cellulose surface or a PDMS cap as presented elsewhere.[23] The surfaces are carefully brought together in such a way that a negative load is obtained. The surfaces are then brought together stepwise in 10 min intervals, until a predetermined maximum load is reached (~250 mg). After 30 min, unloading begins and is performed in the same way as the loading, until the surfaces are pulled apart. No attempts were made in the present work to evaluate the influence of the kinetics of loading and unloading. Because the PDMS lens is transparent, the contact area increase/decrease can be directly imaged through a microscope connected to a computer via a CCD camera. All measurements were performed at 30% or 50% relative humidity (RH) and 23 °C. The adhesion between two elastic bodies can be evaluated using the JKR theory[16] as outlined in eqs 1 and 2. According to eq 1, the JKR theory provides a relationship between the adhesion energy (W), the elastic constant of the system (K), the equivalent radius (R), and the cube of the contact radius (a^3) at a given load (F). When cap/flat geometry is used, R equals the radius of the elastic sphere. In this paper, the R values were about 1 mm. The numerical values of W and K were obtained by fitting the loading data to eq 1.

$$a^3 = \frac{R}{K}[F + 3\pi WR + \sqrt{6\pi WRF + (3\pi WR)^2}] \qquad (1)$$

The adhesion energy at minimum load, W_{min}, is determined from the minimum force obtained from the unloading data (F_s), according to eq 2.

$$F_s = \frac{3}{2}\pi R W_{min} \qquad (2)$$

Results

Surface Characterization. The cellulose films were subjected to surface characterization using contact angle measurements and AFM imaging. Figure 1a−c shows tapping mode AFM height images of the cellulose surfaces (cellulose I, cellulose A, and cellulose B). Both 1 and 100 μm^2 images are presented, which were used to determine the surface roughness as shown in Table 1. The images in Figure 1a−c demonstrate that the structure of all of the films is dominated by round aggregates. The largest aggregates were found on cellulose A (prepared from NMMO/DMSO). Apart from the apparent aggregate dimensions, all of the cellulose surfaces are of a similar structure and, most importantly, continuous and smooth over a large scale (100 μm^2).

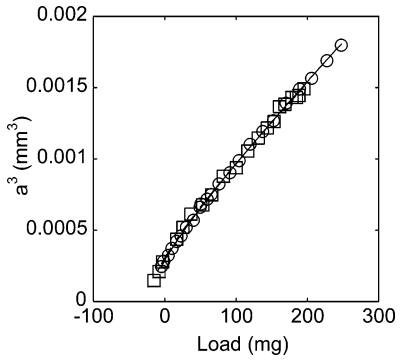

Figure 2. Results from adhesion measurements between two PDMS caps showing the cube of the contact radius as a function of applied loading data. ○ refer to loading data, and □ refer to unloading data. The measurements were performed at 50% RH.

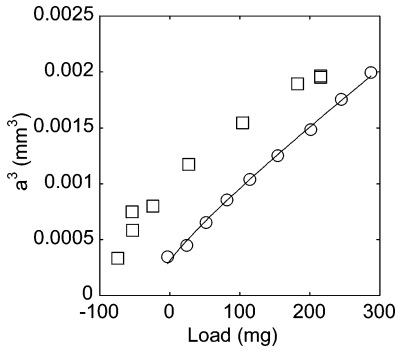

Figure 3. Results from adhesion measurements between two OxPDMS caps showing the cube of the contact radius as a function of applied loading data. The PDMS was treated in the plasma oven for 5 min to obtain OxPDMS. ○ refer to loading data, and □ refer to unloading data. The measurements were performed at 50% RH.

To evaluate the surface chemistry of the surfaces, that is, their ability to engage in specific and nonspecific interactions, the three different cellulose surfaces, as well as the PDMS surface, were characterized through contact angle measurements against both water and methylene iodide. The values obtained are presented in Table 2 together with earlier published data.

Adhesion between PDMS Surfaces. To fully clarify the adhesion between PDMS and cellulose, it was first necessary to investigate the adhesion between PDMS and oxidized PDMS (OxPDMS). This was considered important because cellulose is a polar substrate and unoxidized PDMS is a relatively nonpolar substrate.[17] OxPDMS was obtained by treating the PDMS in a plasma oven for either 1 or 5 min. Three different combinations were investigated: PDMS:PDMS, OxPDMS:OxPDMS, and PDMS:OxPDMS. Both the loading and the unloading data for these three PDMS systems are presented in Figures 2−4. The work of adhesion from loading data (W_A) was calculated using eq 1, and the adhesion energy at minimum load (W_{min}) was calculated using eq 2. Those values are presented in Table 3. If the PDMS caps were oxidized for 1 min, the adhesion force was too strong and a cohesive failure occurred within the PDMS cap. Therefore, the unloading data from these measurements are not presented.

Adhesion between Cellulose and PDMS. Measurements have previously been performed between PDMS and cellulose films prepared by the Langmuir Blodgett technique[17] and the spin-coated semicrystalline cellulose surface (here, surface A)[18] prepared in the same way as in the present investigation.

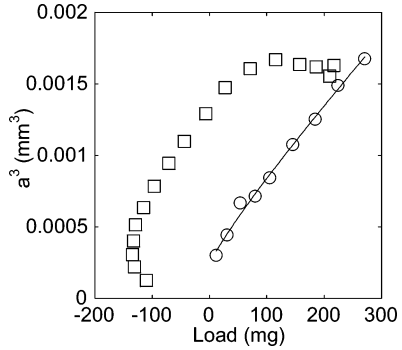

Figure 4. Results from adhesion measurements between one PDMS surface and one OxPDMS surface, showing the cube of the contact radius as a function of applied loading data. ○ refer to loading data, and □ refer to unloading data. The PDMS was treated in a plasma oven for 1 min to give an Ox PDMS surface. The measurements were performed at 50% RH.

Table 3. Summary of the Results from the Adhesion Measurements with PDMS Caps, Showing the Calculated Work of Adhesion from the Loading (W_A)/Unloading Data (W_B), Work of Adhesion from the Pull-Off Force (W_{min}), and Elastic Constants for the Systems (K)[a]

sample	W_A (mJ/m²)	W_B (mJ/m²)	W_{min} (mJ/m²)	K (MPa)
PDMS/PDMS	51 ± 2	54 ± 6	45 ± 5	1.5 ± 0.02
OxPDMS/OxPDMS	67 ± 3			1.4 ± 0.1
OxPDMS/OxPDMS[b]	62 ± 2		245 ± 16	1.5 ± 0.1
OxPDMS/PDMS	53 ± 1		476 ± 8	1.5 ± 0.02

[a] The PDMS caps were oxidized for 1 min unless otherwise stated. The measurements were performed at 50% RH. [b] 5 min oxidation.

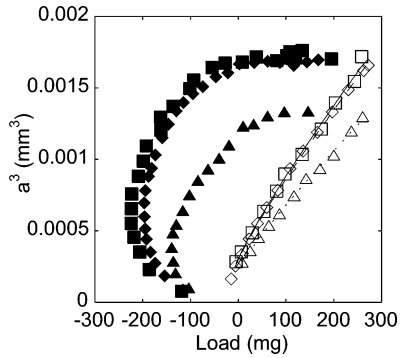

Figure 5. Results from the adhesion measurements between PDMS and cellulose I (triangles), cellulose A (diamonds), and cellulose B (squares) performed at 50% RH, showing the cube of the contact radius as a function of applied loads. Unfilled symbols represent the loading data, while filled symbols represent unloading data.

However, the intention here was to compare different cellulose surfaces for their adhesion behavior. Furthermore, measurements were performed at two different relative humidity values (RH), 30% and 50%, respectively. The adhesion results for those three surfaces against a PDMS cap in 50% and 30% RH are presented in Figures 5 and 6, respectively. From the loading curves, the work of adhesion (W_A) was calculated using eq 1. All values are presented in Table 4, showing no significant difference in the W_A for these different cellulose surfaces, except for surface B (prepared from LiCl/DMAc) in 30% RH. However, there are significant differences in the obtained adhesion hysteresis. This is also evident from W_{min}, calculated from the pull-off force, using eq 2. The calculated data are summarized in Table 4. The obtained adhesion hysteresis is less pronounced at 30% RH when compared to the measurements at 50% RH. This is also clear from the W_{min}, as presented in Table 4. Figure 5 shows that there is a detectable difference in the obtained adhesion

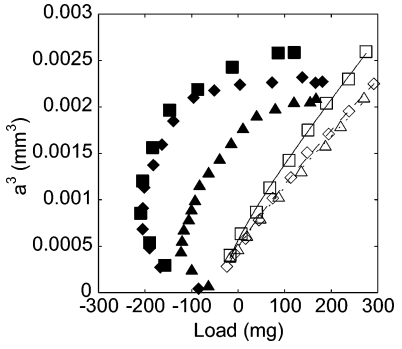

Figure 6. Results from the adhesion measurements between PDMS and cellulose I (triangles), cellulose A (diamonds), and cellulose B (squares) performed at 30% RH, showing the cube of the contact radius as a function of applied loads. Unfilled symbols represent the loading data, while filled symbols represent unloading data.

hysteresis between surfaces A and B at 50% RH. This difference in adhesion hysteresis has disappeared at 30% RH (Figure 6), but it is still clear that the cellulose I surface shows the lowest adhesion hysteresis regardless of the humidity.

Discussion

Surface Characterization. When adhesion measurements are performed, one critical issue is the roughness of the surfaces. Most adhesion measurements with the JKR type of apparatus involve silica surfaces, which are known to be smooth. In this investigation, different cellulose surfaces, with different degrees of crystalline ordering, were prepared on silica surfaces, and the adhesion between these surfaces and PDMS was measured. These cellulose surfaces were shown to have a similar structure with round aggregates. However, surface A had structures that were a bit larger than those for the other two cellulose surfaces. This difference in aggregate size is most likely due to the dissolution process. The dissolution of cellulose in NMMO is known to form a fringe micellar type of arrangement before regeneration to the cellulose II semicrystalline structure in water.[24] The existence of round aggregates can partly be due to the AFM measuring principle where the tip geometry definitely leads to a smoothening of the structure occurring on the surface. This means that sharp edges on the surface will appear as rounded structures. It might also be due to a coexistence of crystalline structure and more amorphous materials, and it has also been shown that a heat treatment of cellullose A surfaces[14] leads to a creation of a more fibrillar structure of the surfaces, that is, a removal of the rounded aggregates. The exact reason for this behavior has not been identified, but it might be speculated that the heat treatment leads to the formation of a more pure crystalline surface and that the initial rounded aggregates are due to the more amorphous materials of the cellulose. This is currently being evaluated with grazing angle X-ray scattering by the authors. Nevertheless, the surfaces were smooth on a nanometer scale as shown by the rms roughness values presented in Table 1.

In the ideal case, the adhesion is determined by the chemical composition of the surfaces, which provide for different types of interactions, such as nonspecific (van der Waal forces) and specific (e.g., hydrogen bonding) interactions. Contact angle measurements using water and methylene iodide were performed to provide information regarding the possibility for dispersive and polar interactions, respectively, for the surfaces used. These values are presented in Table 2. The values for contact angle measurements against methylene iodide ($\gamma_l^d \approx \gamma_l =$

Table 4. Summary of the Results from the Adhesion Measurements with PDMS Caps and Cellulose Surfaces, Showing the Work of Adhesion from the Loading Data (W_A), Work of Adhesion from the Pull-Off Force (W_{min}), and Elastic Constants (K)[a]

	30% RH			50% RH		
sample	W_A (mJ/m^2)	W_{min} (mJ/m^2)	K (MPa)	W_A (mJ/m^2)	W_{min} (mJ/m^2)	K (MPa)
PDMS/cellulose I	49 ± 6	213 ± 32	3.2 ± 0.2	45 ± 4	289 ± 29	3.2 ± 0.2
PDMS/cellulose A	47 ± 3	347 ± 14	2.9 ± 0.2	47 ± 3	389 ± 32	3.1 ± 0.2
PDMS/cellulose B	40 ± 4	337 ± 31	2.7 ± 0.1	46 ± 4	472 ± 32	2.9 ± 0.2

[a] The measurements were performed at 30% or 50% RH, as indicated in the table.

Table 5. Calculated Values for the Dispersive Part of the Surface Energies for the Cellulose Surfaces, PDMS Sheets, and Oxidized PDMS (OxPDMS) Sheets

sample	γ_s^d (mJ/m^2)
cellulose I	42
cellulose A	40
cellulose B	41
PDMS	22
OxPDMS	38

Table 6. Work of Adhesion from Loading Data (W_A), As Determined by JKR-Measurements and the Calculated Dispersive Contributions to the Work of Adhesion (W_{12}^d)[a]

system	30% RH W_A (mJ/m^2)	50% RH W_A (mJ/m^2)	W_{12}^d (mJ/m^2)
PDMS/PDMS	51 ± 2		44
PDMS/OxPDMS	53 ± 1		57
OxPDMS/OxPDMS	67 ± 3		75
PDMS/cellulose I	49 ± 6	45 ± 4	61
PDMS/cellulose A	47 ± 3	47 ± 3	59
PDMS/cellulose B	40 ± 4	46 ± 4	60

[a] The PDMS caps were oxidized for 1 min.

50.8 mJ/m^2) were used to calculate the dispersive part of the surface energy (γ_s^d) according to eq 3, which is valid when the interactions between the liquid and the surface are dominated by dispersive interactions.[25]

$$2\sqrt{\gamma_s^d \gamma_l^d} = \gamma_l(1 + \cos\Theta) \quad (3)$$

All calculated values are presented in Table 5. These values indicate that the dispersive part of the cellulose surface energy is dominating over the polar contribution, because the surface energy of cellulose is known to be around 54.5 mJ/m^2 determined by contact angle measurements.[25] Reported values for the dispersive part of the surface energy of cellulose are 40 and 44.0 mJ/m^2, determined by contact angle measurements.[18,25] These values are similar to the values in the present investigation. The dispersive part of the PDMS surface energy is also in agreement with previous studies showing values around 21−22.5 mJ/m^2, as determined with contact angle measurements.[26]

Work of Adhesion from Dispersive Interactions. By using the data in Table 5, it was possible to calculate the work of adhesion due to the dispersive interaction (W_{12}^d) between the investigated systems according to eq 4.

$$W_{12}^d = 2\sqrt{\gamma_1^d \gamma_2^d} \quad (4)$$

A summary of these calculations and the experimental values obtained with contact mechanics is presented in Table 6 and will be further discussed below.

Adhesion between PDMS Caps. The energy needed to separate two surfaces is very often higher than that needed to bring them together. This is observed when comparing loading and unloading data. The origin of this hysteresis has been attributed to have several causes such as inter-diffusion and hydrogen bonding.[27−29] When two PDMS surfaces are studied, as in Figure 2, there is no detectable adhesion hysteresis. This is expected and has been shown in other investigations.[17,26,29] Both loading and unloading data could be fit to the JKR theory using eq 1. The W_A was found to be 50.5 ± 2.2 mJ/m^2. The work of adhesion for the unloading data (W_B) shows a somewhat higher value, 54.4 ± 6.3 mJ/m^2, indicating a small adhesion hysteresis. When either or both PDMS surfaces were oxidized in a plasma oven, a significant adhesion hysteresis was obtained, as shown in Figures 3 and 4. This has been described earlier, but to the best knowledge of the authors the adhesion between one plasma-treated and one non-treated cap has not been published previously. When both surfaces were oxidized for 1 min, the adhesion detected from the unloading curve was very strong, indicating cohesive failure, and was out of the limit for the evaluation principles used in the present work. This behavior was also detected by Chaudhury et al.[26] If both PDMS surfaces were subjected to the plasma treatment for a longer time, here 5 min, the adhesion was again measurable, showing an adhesion hysteresis more similar to the results presented by Rundlöf et al.[17] These differences are suggested to be due to the possibility of forming a glass layer on the PDMS surface with the longer time in the plasma oven, specially for the surfaces treated for 5 min. This in turn will make the surface less elastic and decrease the mobility of the surface molecules as well as the adhesion. The W_A in the present work was 67.0 ± 3.2 mJ/m^2 (1 min oxidation) and 61.5 ± 1.7 mJ/m^2 (5 min oxidation), respectively. This increase in W_A as compared to the values for the untreated PDMS caps has been seen in other investigations, and even higher values up to 117 mJ/m^2 have been reported.[26] When one of the PDMS surfaces was subjected to the plasma for 1 min and the adhesion was measured against one untreated PDMS surface, the calculated W_A had an intermediate value of 53.2 ± 0.3 mJ/m^2. If the dispersive component of the work of adhesion (W_{12}^d) is compared to the W_A obtained from the JKR measurements (Table 6), it seems that the W_A mainly consists of dispersive interactions, which has also been discussed previously.[23,26] However, the dispersive interactions, as determined by contact angle measurements, have somewhat higher values than those determined by JKR measurements, but are still in fairly good agreement. Furthermore, the polar part of the interaction also increases with plasma treatment of PDMS, that is, introduction of OH groups,[17] as shown from contact angle measurements against water (Table 2). The contact angles for a PDMS sheet toward water are about 110°, and subjecting them to plasma treatment lowers it to around 0°. This in turn makes it natural to ascribe the adhesion hysteresis, when either or both PDMS caps are subjected for plasma treatment, to be due to hydrogen bonding, as previously suggested.[17,26,29]

Adhesion between PDMS Caps and Cellulose. The W_A between PDMS and cellulose I, cellulose A, and cellulose B

did not differ to any large extent, as shown in Table 6. From this table, it can be concluded that there are no significant differences in the W_A, as determined by JKR measurements, or the W_{12}^d, as calculated from contact angle measurements for values obtained at 50% RH. This suggests that the W_A mainly consists of dispersive interaction forces. For measurements performed at 30% RH, there are indications that the ordering of the cellulose plays a role, showing higher W_A for surfaces containing regions with higher crystalline order. In addition, as is shown in Figures 5 and 6, there are significant differences in the development of the adhesion hysteresis, as well as the W_{min}, presented in Table 4. These results suggest that there is a correlation between the degree of ordering of the cellulose surface and the measured adhesion hysteresis against a PDMS cap. Furthermore, this hysteresis is influenced by the RH. This difference is suggested to depend on the ability of the interfacial molecules on the cellulose surfaces to orient in such a way that specific molecular interaction can occur. A cellulose surface containing less ordered regions (surfaces A and B) showed a larger adhesion hysteresis and W_{min} than did the cellulose I surface. This indicates that a cellulose surface with less ordered parts has higher possibility to orient its surface groups and hence achieve molecular interactions with the PDMS surface. In addition, increasing the RH from 30% to 50% resulted in a larger adhesion hysteresis. Possibly due to the surface's ability to take up water, consequently there will be a higher water uptake at the higher humidity, leading to a larger mobility of the surface molecules. The water uptake will also plasticize the cellulose surfaces and contribute to the development of molecular contact between the surfaces. At 50% RH, one can also detect a difference in the obtained adhesion hysteresis between surfaces A and B (Figure 5), which was not possible from the measurements at 30% RH, as shown in Figure 6. This further supports the hypothesis that the water uptake will highly influence the formation of the joint and the obtained adhesion hysteresis and that a stronger joint is formed when the surfaces have a higher degree of water uptake. Furthermore, this can be an indication that surface A indeed has a higher degree of ordering than does cellulose B. These measurements indicate that, as the surfaces are pressed against each other, dispersive interactions dominate, and when the surfaces are separated, after being held in contact for a predetermined time, additional forces have to be considered, and in this system, hydrogen bonding is suggested to contribute to the adhesion hysteresis.

Another factor that might affect the measurements is the influence on moisture on surface roughness. The surface roughness values shown in Table 1 were collected at 50% RH, and a change in humidity might change this roughness. However, as the change in absorption of water is not dramatic in this humidity interval, it is not anticipated that a change in surface structure might be the cause of the detected differences. Furthermore, a large change in surface roughness would also show up as a change in work of adhesion upon loading, and the largest differences in Table 4 are definitely detected for the unloading experiments in the MAMA experiments.

Because the measurements were performed in a humid environment, it is important to discuss the possibility of forming capillary condensation between the surfaces. From an investigation using the AFM colloidal probe technique, it was shown that between two cellulose surfaces a distinct increase in the adhesion was detected at 60% RH.[30] With this as a background, it is suggested that the achieved adhesion in these measurements is not likely due to capillary condensation. Regardless, the water will have a significant influence on the adhesion, as already discussed.

From earlier investigations, where the adhesion between PDMS and LB-cellulose/semicrystalline cellulose (surface A in this investigation) has been studied, the obtained values have been shown to be of similar magnitude.[17] The measurement using the LB-cellulose film was performed under conditions ranging from 33% to 47% RH. Therefore, it is difficult to compare those results with the present investigation. However, the values are similar to the ones presented here, and the W_A was between 47.4 and 51.6 mJ/m^2 and W_{min} was 201 mJ/m^2. The semicrystalline surface measurement was performed at a RH of 50% and can thus be directly compared to the present measurement showing similar values of W_A (43 mJ/m^2) and W_{min} (400 mJ/m^2). These values should be compared to 47 ± 3 and 390 ± 32 mJ/m^2, respectively, in the present investigation.

It should be mentioned that for these kinds of measurements there are many factors contributing to the differences in the obtained results, for example, storage time of surfaces, storage conditions, and the way of handling surfaces. The cellulose surfaces used in the present investigation also have a different thickness ranging from 30 nm (cellulose A) to 120 nm for the cellulose I surface. It is well accepted the in-plane properties of thin films are significantly different from those of bulk materials from the same chemical material. It is also well accepted that surface molecules have restrictions different from those bulk molecules of the same material. However, these are not the properties tested and discussed in the present work; furthermore, it is well known that van der Waals interactions are dominated by the most external layers of the material, and therefore it is not anticipated that the difference in thickness of the present materials will be important for the measured interactions. However, this will be checked in future investigations.

It should also be mentioned that pull-off forces do vary considerably if the same surfaces are tested repeatedly.[31,32] Nevertheless, there are clear differences in the present investigation, and the results clearly indicate that the degree of crystalline ordering of the cellulose surfaces is important for the adhesion, which are engaging for further investigations.

Conclusion

The use of the microadhesion measurement apparatus (MAMA) for studying the adhesion between PDMS and cellulose surfaces was demonstrated. All investigated cellulose surfaces showed roughly the same work of adhesion from loading data (W_A), as determined by JKR theory. From contact angle measurements, the dispersive contribution to the W_A could be calculated, showing similar values, indicating that the adhesive interactions were dominated by dispersive interactions for the loading data. However, there were clear differences when the adhesion hysteresis (unloading data) and the adhesion energy at minimum load (W_{min}) (as calculated from the minimum forces) were studied. A cellulose surface prepared from nanocrystals gives rise to a lower adhesion hysteresis and lower W_{min} than a less ordered cellulose surface, prepared from dissolved cellulose. This is suggested to depend on the higher possibility for the less ordered regions to orient their surface groups and form specific interactions with the surface groups on the PDMS surface. Furthermore, an increase in the relative humidity resulted in a larger adhesion hysteresis and W_{min}, which probably originates from the surfaces possibility to take up water, thereby

increasing the mobility of the surface molecules, and possibly water acts as a plasticizer, contributing to a stronger joint. Again, the less ordered surfaces showed the largest adhesion hysteresis and W_{min}, which can be explained by its water uptake.

Acknowledgment. M.E. acknowledges KTH, Royal Institute of Technology, and the Lyckeby Industrial Research Foundation for financial support. S.M.N. would like to acknowledge the Co-operative Research Centre for Functional Communication Surfaces (CRC SmartPrint) for financial support.

References and Notes

(1) Lindström, T.; Wågberg, L.; Larsson, T. *13th Fundamental Research Symposium*; Cambridge, UK, 2005.
(2) Van Oss, C. J.; Chaudhury, M. K.; Good, R. J. *Adv. Colloid Interface Sci.* **1987**, *28*, 35.
(3) Israelachvili, J. *Intermolecular and Surface Forces*; Academic Press: New York, 1991.
(4) Gunnars, S.; Wågberg, L.; Cohen Stuart, M. A. *Cellulose (Dordrecht, Netherlands)* **2002**, *9*, 239.
(5) Gunnars, S.; Wågberg, L.; Cohen Stuart, M. A. *Cellulose (Dordrecht, Netherlands)* **2003**, *10*, 185.
(6) Edgar, C. D.; Gray, D. G. *Cellulose (Dordrecht, Netherlands)* **2003**, *10*, 299.
(7) Holmberg, M.; Berg, J.; Stemme, S.; Ödberg, L.; Rasmusson, J.; Claesson, P. *J. Colloid Interface Sci.* **1997**, *186*, 369.
(8) Zauscher, S.; Klingenberg, D. J. *J. Colloid Interface Sci.* **2000**, *229*, 497.
(9) Eriksson, J.; Malmsten, M.; Tiberg, F.; Callisen, T. H.; Damhus, T.; Johansen, K. S. *J. Colloid Interface Sci.* **2005**, *284*, 99.
(10) Notley, S. M.; Pettersson, B.; Wågberg, L. *J. Am. Chem. Soc.* **2004**, *126*, 13930.
(11) Rutland, M. W.; Carambassis, A.; Willing, G. A.; Neuman, R. D. *Colloids Surf., A* **1997**, *123*−*124*, 369.
(12) Österberg, M. *J. Colloid Interface Sci.* **2000**, *229*, 620.
(13) Österberg, M.; Claesson, P. M. *J. Adhes. Sci. Technol.* **2000**, *14*, 603.
(14) Notley, S. M.; Wågberg, L. *Biomacromolecules* **2005**, *6*, 1586.
(15) Carambassis, A.; Rutland, M. *Langmuir* **1999**, *15*, 5581.
(16) Johnson, K. L.; Kendall, K.; Roberts, A. D. *Proc. R. Soc. London, Ser. A* **1971**, *324*, 301.
(17) Rundlöf, M.; Karlsson, M.; Wågberg, L.; Poptoshev, E.; Rutland, M.; Claesson, P. *J. Colloid Interface Sci.* **2000**, *230*, 441.
(18) Forsström, J.; Eriksson, M.; Wågberg, L. *J. Adhes. Sci. Technol.* **2005**, *19*, 783.
(19) Notley, S. M.; Eriksson, M.; Wagberg, L.; Beck, S.; Gray, D. G. *Langmuir* **2006**, *22*, 3154.
(20) Fält, S.; Wågberg, L.; Vesterlind, E. L.; Larsson, P. T. *Cellulose (Dordrecht, Netherlands)* **2004**, *11*, 151.
(21) Berthold, F.; Gustafsson, K.; Berggren, R.; Sjöholm, E.; Lindström, M. *J. Appl. Polym. Sci.* **2004**, *94*, 424.
(22) Sjöholm, E.; Gustafsson, K.; Pettersson, B.; Colmsjö, A. *Carbohydr. Polym.* **1997**, *32*, 57.
(23) Dillard, D. A.; Pocius, A. V.; Chaudhury, M. K. *Adhesion Science and Engineering*; Elsevier: Amsterdam, Boston, 2002.
(24) Arndt, K.-F.; Morgenstern, B.; Röder, T. *Macromol. Symp.* **2000**, *162 (Data Evaluation in Light Scattering of Polymers)*, 109.
(25) Van Oss, C. J. *Interfacial Forces in Aqueous Media*; M. Dekker: New York, 1994.
(26) Chaudhury, M. K.; Whitesides, G. M. *Langmuir* **1991**, *7*, 1013.
(27) Leckband, D.; Chen, Y. L.; Israelachvili, J.; Wickman, H. H.; Fletcher, M.; Zimmerman, R. *Biotechnol. Bioeng.* **1993**, *42*, 167.
(28) Luengo, G.; Pan, J.; Heuberger, M.; Israelachvili, J. N. *Langmuir* **1998**, *14*, 3873.
(29) Kim, S.; Choi, G. Y.; Ulman, A.; Fleischer, C. *Langmuir* **1997**, *13*, 6850.
(30) Stiernstedt, J. Doctoral Thesis, KTH, Stockholm, Sweden, 2006.
(31) Claesson, P. M.; Dedinaite, A.; Rojas, O. J. *Adv. Colloid Interface Sci.* **2003**, *104*, 53.
(32) Kendall, K. *Molecular Adhesion and Its Applications: The Sticky Universe*; Kluwer Academic/Plenum Publishers: New York, 2001.
(33) Ginn, B. T.; Steinbock, O. *Langmuir* **2003**, *19*, 8117.

BM061164W